CrossMark

ORIGINAL PAPER

Dynamic analysis of double wishbone front suspension systems on sport motorcycles

Ciro Moreno Ramírez⬤ · **M. Tomás-Rodríguez** ·
Simos A. Evangelou

Abstract In this paper, two alternative front suspension systems and their influence on motorcycle nonlinear dynamics are investigated. Based on an existing high-fidelity motorcycle mathematical model, the front end is modified to accommodate both Girder and Hossack suspension systems. Both of them have in common a double wishbone design that varies the front end geometry on certain manoeuvrings and, consequently, the machine's behaviour. The kinematics of the two systems and their impact on the motorcycle performance are analysed and compared to the well-known telescopic fork suspension system. Stability study for both systems is carried out by combination of nonlinear dynamical simulation and root-loci analysis methods.

Keywords Motorcycle · Vehicle dynamics · Mathematical modelling · Stability analysis · Suspension systems

C. Moreno Ramírez (✉)
Departamento de Ingeniería Industrial y Automoción - E.P.S., Universidad Antonio de Nebrija, Madrid, Spain
e-mail: CMorenoRa@Nebrija.es

M. Tomás-Rodríguez
Department of Mechanical Engineering and Aeronautics, City, University of London, London, UK
e-mail: Maria.Tomas-Rodriguez.1@city.ac.uk

S. A. Evangelou
Electrical and Electronic Engineering Department, Imperial College London, London, UK
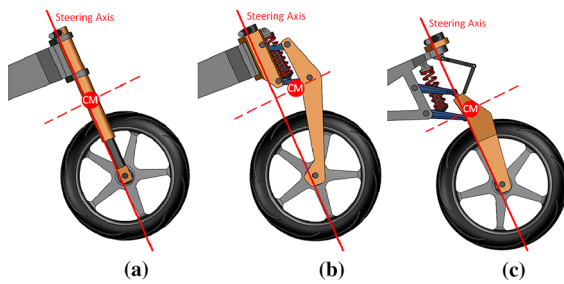e-mail: S.Evangelou@imperial.ac.uk

1 Introduction

The motorcycle's front end links the front wheel to the motorcycle's chassis and has two main functions: the front wheel suspension and the vehicle steering. Up to this date, several suspension systems have been developed in order to achieve the best possible front end behaviour, being the telescopic fork the most common one.

A telescopic fork 3D model can be observed in Fig. 1a. It consists of a couple of outer tubes which contain the suspension components (coil springs and dampers) internally and two inner tubes which slide into the outer ones allowing the suspension travel. The outer tubes are attached to the frame through two triple trees which connect the front end to the main frame through the steering bearings and allow the front wheel to turn about the steering axis. This system keeps the front wheel's displacement in a straight line parallel to the steering axis. However, there exist alternative suspension designs that allow different trajectories of the front wheel with the suspension travel. An extensive review of most of the existing alternatives suspension systems can be found in [10], in which their advantages and drawbacks in relation to each other are explained. This reference classifies front suspension systems into two main groups depending on how they are connected to the main frame: head stock mounted fork and alternatives systems. In the present research, the different suspension systems are classified in a different manner

Fig. 1 3D models of Fork (**a**), Girder (**b**) and Hossack (**c**) suspension systems. Centres of masses and steering axis are shown with red dots and lines, respectively. (Color figure online)

considering kinematics criteria. Two different groups can be defined depending on the steering axis' location in the suspension assembly. The first group comprises those systems which present the steering axis located between the chassis and the suspension elements (pivoted arms or wishbones in most of the cases). In the second group, this axis is placed between the suspension elements and the front wheel. In both cases, the system can be designed in order to provide a desired front wheel trajectory, however whilst the first group keeps the steering angle fixed in the chassis reference frame, the second one modifies it with the travel of the suspension.

A deep study of four alternative suspension systems belonging to the second group of this later classification (two Hub-centre systems and two Dual-link systems) can be found in [13]. The authors investigate their effects on motorcycle dynamics taking advantage of advanced multi-body software (namely Simpack) and performing several running simulations close to real driving conditions. For the four different suspension systems, various aspects of the motorcycle response, such as the forces transmitted to the suspension joints, the resulting bending torque on the frame's lateral axis, the pitch angle achieved by the motorcycle or the maximum roll velocity are studied as a means to understand the advantages of each system under different design considerations.

In the present research, our main goal is to study the effects of alternative front suspension systems of both groups defined above, not only in terms of motorcycle response but also in terms of motorcycle dynamics and stability. That is, how the different modifications introduced by the new suspension systems, such as different mechanical designs or changes in the front end geometry with new wheel trajectories, affect the sus-

pension response and the motorcycle's oscillating normal modes.

Two double wishbone systems are considered in this research as representative of these two groups: the Girder suspension and the Hossack system, respectively. In terms of kinematics, these two types of designs cover most of the existing double wishbone suspension systems. 3D models of these suspension systems are shown in Fig. 1. The Girder suspension system (Fig. 1b) consists of a pair of long uprights where the front wheel is attached to. These uprights are linked to the triple trees by an upper and a lower wishbones which perform the suspension motion. Both triple trees rotate about the steering axis which is fixed to the motorcycle chassis. A spring-damper unit is usually attached between the lower wishbone and the upper triple tree providing the shock absorption function. On the other hand, the Hossack suspension system (Fig. 1c) consists of a double wishbone structure directly attached to the chassis. The two wishbones rotate both about axes perpendicular to the symmetry plane of the motorcycle, providing the suspension motion. An upright is linked to the front tips of the wishbones by two ball joints, which allow it to turn left and right as well as to move up and down. Therefore, the steering axis becomes defined by the imaginary line passing through the geometric centre of the ball joints. The control over the steering angle is applied by the rider to the handlebar which is connected to the upright through the steering linkage. This is a system of two levers, connected by an axis, which can be compressed or elongated in order to reach the length between the handlebar and the upright. The front wheel is attached to this upright, and the suspension reaction is provided by a spring-damper unit attached between the lower wishbone and the motorcycle chassis.

The framework of this research is the mathematical modelling and numerical simulation. We took advantage of a high-fidelity motorcycle model developed by [23] which has been modified with the addition of the alternative suspension system under study. The motorcycle model properties and the simulation tools used during this research are explained in Sect. 2. In order to obtain realistic descriptions of the alternative front suspension systems in terms of dynamical properties, we have designed and modelled these systems taking advantage of CAE tools. As a first step, the kinematics of the two systems are studied in comparison with the telescopic fork. Then, different kinematic configu-

rations are synthesized taking into consideration different aspects of the front end geometry. This part of the research is explained in Sect. 3. The second step consists in 3D design and compliance analysis of the suspension systems. This process allows to obtain realistic values for the dynamical properties (such as masses and moments of inertia) of the suspension systems' parts. Once the dynamical properties of all the suspension systems' parts are obtained, the motorcycle model was modified to include the new suspension systems. This dynamical modelling process is explained in Sect. 4. Several simulations were carried out with the new motorcycle models in order to test the suspension response under different conditions (Sect. 5). Full stability analyses were performed to identify and reduce the eventual stability risks that the new suspension systems may introduce in the motorcycle dynamics (Sect. 6). Finally, conclusions of this research are presented in Sect. 7.

2 Motorcycle model and simulation tools

The different mathematical models developed for this research are based on the model presented in [23]. This mathematical model was built during several years of research underpinned by wide literature and experimental data. This model has been extensively used in the past in several contributions such as [5–7,18,21,22]. Furthermore, it has been widely tested and adopted by the industry. For instance, BikeSim software [14] is a motorcycle dynamics simulator which is based on this model and it is used by a large number of manufacturers to obtain high-fidelity prediction on the dynamics of their machines.

The model was developed using real dynamical parameters of an existing motorcycle. The Suzuki GSX-R1000 K1 superbike, with 170 kg of mass, powered by an in-line four cylinder and four stroke engine with 988 cc able to deliver 160 hp, this machine is a good representative of contemporary commercial high-performance motorcycles.

The motorcycle model consists of seven bodies: rear wheel, swinging arm, main frame (comprising rider's lower body, engine and chassis), rider's upper-body, steering frame, telescopic fork suspension and front wheel. It involves 13 degrees of freedom: three rotational and three translational for the main frame, two rotational for the wheels spin, one rotational for the
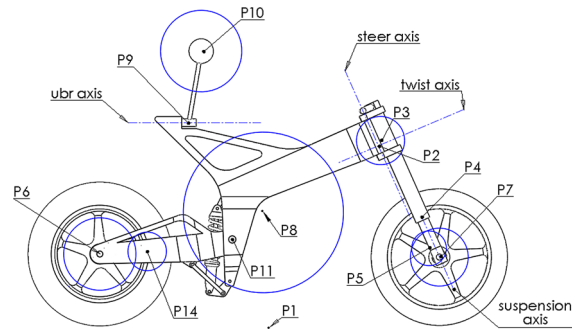

Fig. 2 GSX-R1000 geometrical description. Blue circles with diameter proportional to body mass are plotted around the centre of mass of each body. (Color figure online)

Table 1 GSX-R1000 geometrical model main points

Point	Description
P1	Aerodynamic reference point
P2	Twist body's joint with rear frame
P3	Steer body's centre of mass
P4	Front suspension body's joint with steer body
P5	Front suspension body's centre of mass
P6	Rear wheel's centre of mass and attachment point
P7	Front wheel's centre of mass and attachment point
P8	Main frame's centre of mass
P9	Rider's upper body attachment point on rear frame
P10	Centre of mass of the rider's upper body
P11	Swinging arm's attachment point on main frame
P14	Swinging arm's centre of mass

swinging arm, one rotational for the rider's upper body, one rotational for the frame flexibility, one rotational for the steering body and one translational for the front suspension fork. Figure 2 represents the main geometric points and axes in the motorcycle's geometry. The centre of mass of each of the seven constituent bodies is represented as a blue circle with a diameter proportional to its mass. Table 1 contains the indexes of these points. For modelling purposes, a parent–child structure is used, as shown in Fig. 3.

The tires are treated as wide, flexible in compression and the migration of both contact points as the machine rolls, pitches and steers is tracked dynamically. The tyre's forces and moments are generated from the tyre's camber angle relative to the road, the normal load and the combined slip using Magic Formu-
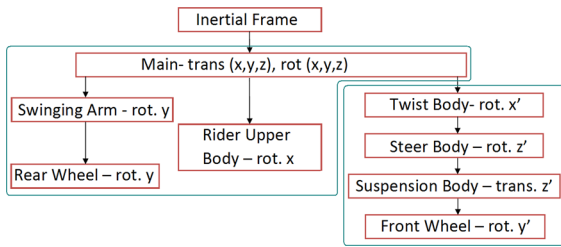
Fig. 3 Parental structure of the GSX-R1000 model

lae models [15,16]. This model is applicable to motorcycle tires operating at roll angles of up to 60°.

The aerodynamic drag/lift forces and pitching moment are modelled as forces/moments applied to the aerodynamic centre, and they are proportional to the square of the motorcycle's forward speed. In order to maintain steady-state operating conditions, the model contains a number of control systems, which mimic the rider's control action. These systems control the throttle, the braking and braking distribution between the front and rear wheels, and the vehicle's steering.

The forward speed is maintained by a driving torque applied to the rear wheel and reacting on the main frame. This torque is derived from a proportional–integral (*PI*) controller on the speed error with fixed gains.

For some manoeuvres, the motorcycle is not self-stable; in order to stabilize the machine in such situations a roll angle feedback controller is implemented. This allows to obtain different steady turning equilibrium states through simple simulations, which will not be stable without the roll angle controller. The controller developed was a proportional–integral–derivative (*PID*) feedback of motorcycle lean angle error to steering torque. The lean angle target is set by an initial value and a constant change rate. Thus, the target lean angle is a ramp function of time which can be easily modified. The *PID* gains are defined as speed adaptive in order to achieve an effective stabilization of the motorcycle for the difficult cases involving very low or very high speeds. Finally, the steering control torque is applied to the steer body reacting on the rider's upper body.

Some modification to the baseline model has been applied for this research regarding the acceleration/braking systems and road inputs. In order to study the response of the new suspensions and their anti-dive properties, a braking system capable of delivering a constant deceleration was implemented. In the new sys-

tem, the braking torque is derived from the PI controller on the speed error. On the other hand, the road input into the motorcycle tyres is also redefined. With the new approach, the longitudinal contact point migration produced by a step bump is included in the dynamic description and its effects on the suspension response are considered.

The motorcycle model is implemented taking advantage of the VehicleSim multi-body software from Mechanical Simulation Corporation [14]. This suite consists of two separated tools: VS Lisp and VS Browser. VS Lisp is the tool used to generate the equations of motions from a multi-body description of any dynamical system. Making use of its own computer language (based on LISP), it is designed to automatically generate computationally efficient simulation programs for those multi-body systems. It can be configured to return either the corresponding nonlinear equations of motion or the linearized equations of motion. Both nonlinear and linearized equations of motion are symbolically described as functions of all the parameters defining the model dynamics, such as suspensions or aerodynamics coefficients.

With the nonlinear equations of motion, a solver can be built with the same architecture and behaviour as those existing in commercial packages such as BikeSim and fully compatible with the VS Browser. VS Browser is the front end of all the VehicleSim products. It provides a graphical context with a standard graphical user interface from which the nonlinear simulations can be run and the different databases can be managed. This includes the solvers created with VS Lisp, the external inputs and events and the data post-processing and visualization.

On the other hand, the linearized equations of motion are returned in a MATLAB file with the state space description of the systems. The state space matrices obtained (A, B, C and D) depend on both the system parameters and the state variables values. This feature become useful in the stability analysis of complex nonlinear systems, which can be linearized about operating points corresponding to quasi-equilibrium states. The frequency and damping associated to the system's normal modes are found through the eigenvalues of matrix A. The previous version of this software was called Autosim and was already used in the past in motorcycles multi-body modelling (see [4,19]).

In this research, following the approach of previous works such as [6] or [9], the system's eigenvalues are

plotted in the complex plane for different values of the motorcycle speed and roll angle. In this way a general understanding on the stability properties of the different motorcycle models can be obtained. To do so, the non-linear equations of motions returned by VS Lisp are integrated under a quasi-equilibrium variation of the forward speed to obtain time histories of the state variables, for either straight running conditions or steady turns. Then, the state space matrix A can be fed with those values of the state variables for each time step, obtaining an accurate linear description of the motorcycle system for different forward speeds and roll angles. Speed and roll angle feedback controllers are used to reach the equilibrium states during the nonlinear simulation. However, in the model's state space description these feedback controls are disabled in order to study the open-loop system stability. In Sect. 6 this technique is used to study the variation in the root locus of the motorcycle model introduced by double wishbone suspension systems, that is, the effects on the stability of the motorcycle and its normal modes.

3 Front end kinematics

Motorcycle handling properties are greatly influenced by some geometric parameters which are defined by the front end design. Figure 4 presents the four most relevant geometric parameters for motorcycle handling. These are the trail (t), the normal trail (t_n), the head angle (ε) and the wheelbase (wb). The wheelbase is the distance between the front and rear wheels contact points. The head angle is the angle between the steering axis and the vertica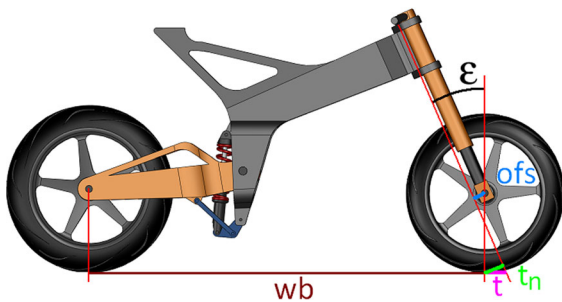l. The trail is the distance between the front wheel contact point and the point where the steering axis intersects with the ground. Finally, the normal trail is the projection of the trail distance into a plane perpendicular to the steering axis. This is the lever arm of the front tyre forces appearing on its contact point, which result in a torque about the steering axis. The normal trail (t_n) and the head angle (ε) are related to each other by the following expression:

$$t_n = r_{fw} \cdot \sin(\varepsilon) - \text{ofs} \tag{1}$$

where r_{fw} is the tyre's radius and ofs is the front wheel's spindle offset from the steering axis. The wheelbase also depends on the rear frame construction including the swinging arm.

In the case of a conventional telescopic fork, the steering axle is rigidly inserted into the chassis whilst the offset is a constant value. Therefore, when the fork is compressed the wheelbase and the head angle decrease and, thus, the trail and the normal trail.

The vertical suspension travel (*v.s.t.*) is defined as the vertical travel of the front wheel centre when the suspension system is compressed (*v.s.t.* > 0) or extended (*v.s.t.* < 0) considering the chassis fixed in the inertial frame. This definition is valid for all the different suspension systems and provides a general magnitude that can be used to compare various behaviours.

Both Girder and Hossack systems consist in a four-bar linkage. The difference between them is the edge of the quadrilateral to be considered as steering axis. Figure 5 shows the design parameters of the four-bar linkage for these two systems: the lengths of the upper (l_1) and lower (l_2) wishbones, the distances between the attachment points of the wishbones (h_1 on the chassis side and h_2 on the uprights side) and the angle between
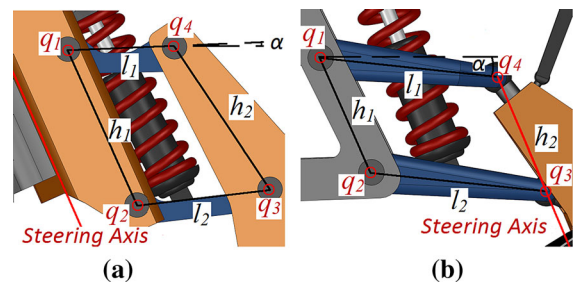

Fig. 4 Main motorcycle's handling geometric parameters. The wheelbase (wb) is plotted in brown, the trail (t) is in magenta, the normal trail (t_n) is in green, the head angle (ε) is in black and the fork offset (ofs) is shown in blue. (Color figure online)

Fig. 5 Design parameters on the four-bar linkage suspension systems. **a** Girder suspension system. **b** Hossack suspension system
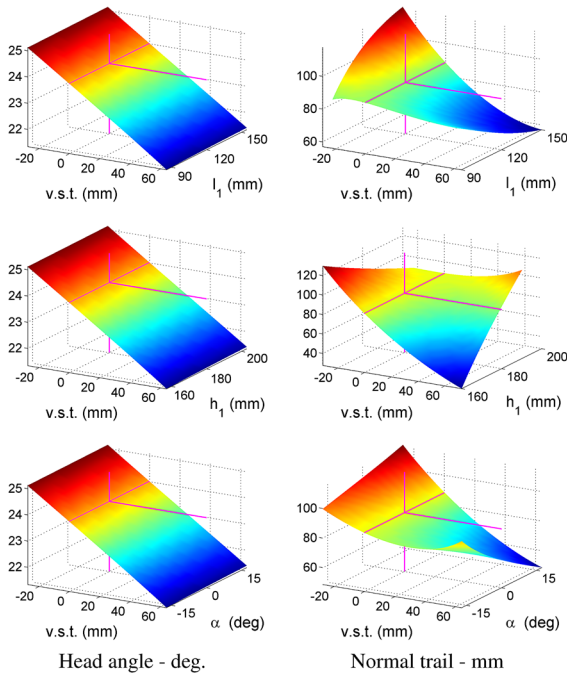
Fig. 6 Effects of varying the design parameters on the head angle and the normal trail for the **Girder** suspension system
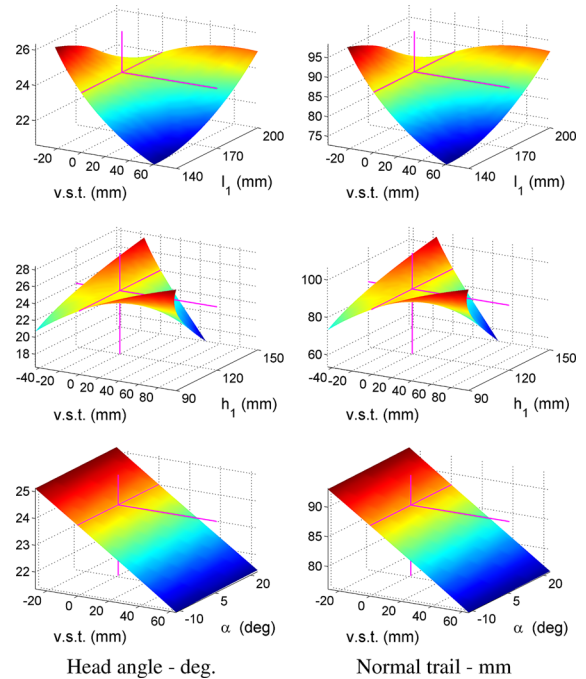

Fig. 7 Effects of varying the design parameters on the head angle and the normal trail for the **Hossack** suspension system

the upper wishbone and the horizontal at the nominal position (α). With these five parameters full assembly kinematics are defined. The variation of one of them will affect the overall behaviour of the handling geometric parameters with the suspension travel. Different configurations of these five parameters can be calculated to obtain different behaviours of the front suspension systems.

The impact on the kinematic behaviour of varying each design parameter value on the handling geometric parameters can be mapped. As an example, Fig. 6 shows the effects of modifying l_1, h_1 and α parameters on the variation, with the vertical suspension travel, of the head angle and the normal trail for the Girder suspension system. Only the normal trail will be taken into consideration as it is the actual lever arm of the front wheel force about the steering axis, whilst the trail can be obtained as a simple function of the former as:

$$t = \frac{t_\mathrm{n}}{\cos(\varepsilon)} \tag{2}$$

As it can be expected, as the steering axis is fixed to the chassis, the head angle variation behaves similarly with different values of any of the design parameters.

However, the normal trail variation is affected by these parameters values. The Girder suspension system can be designed to perform a prescribed behaviour of the wheelbase and the normal trail whilst the head angle behaviour cannot be modified.

Similar results are shown in Fig. 7 for the Hossack system. In this case, a close relation between the head angle and the normal trail behaviours can be observed due to the variable steering axis and the constant offset. The head angle and the normal trail keep their nominal response for different values of α but are significantly modified when other design parameters are varied. It is possible to obtain a desired head angle variation given certain vertical suspension travel with the Hossack suspension system, whilst the trail and the normal trail are closely related to it.

As it has been said, double wishbone suspension systems can be design with different kinematic behaviours. In order to study the effect of the front suspension systems' kinematic behaviour on the motorcycle dynamics, three main kinematic configurations are considered for both the Girder and Hossack suspension systems. The design parameters required for each of these configurations were obtained by means of synthesis of

Table 2 Design parameters values obtained for the three different configurations of the Girder suspension systems

Girder configurations	l_1	l_2	h_1	h_2	α
Parallelogram	120	120	180	180	0.0
Fork trajectory	107	135	171	172	0.0
Constant t_n	106	131	192	185	0.0

l_1, l_2, h_1 and h_2 are expressed in mm and α is expressed in °

Table 3 Design parameters values obtained for the three different configurations of the Hossack suspension systems

Hossack configurations	l_1	l_2	h_1	h_2	α
Parallelogram	170	170	120	120	5.7
Fork trajectory	155	183	127	117	5.8
Constant t_n	173	190	102	123	6.0

l_1, l_2, h_1 and h_2 are expressed in mm and α is expressed in °

mechanisms methodology. Several optimization processes were developed for the different suspension systems taking advantage of MATLAB's optimization toolbox, which was proven to be an adequate framework for this kind of problems. The following kinematic configurations were obtained:

- *Parallelogram* (*prl*) The suspension systems are designed with l_1, l_2, h_1 and h_2 as two pairs of parallel sides and with $\alpha = 0$, being this the simplest configuration. No optimization process is needed and the parallelogram's sides lengths are chosen within the space restrictions imposed by the motorcycle's design.
- *Telescopic fork's trajectory* (*tft*) The suspension systems are designed to obtain a front wheel trajectory similar to that followed by the front wheel with a telescopic fork system.
- *Constant normal trail* (*cnt*) The suspension systems are designed to obtain a constant normal trail along the full suspension travel.

The values of the design parameters obtained are given in Tables 2 and 3, where l_1, l_2, h_1 and h_2 are expressed in mm and α is in °.

Figure 8a shows the handling geometric parameters behaviour of the Girder (green +) and Hossack (red ×) suspension systems with parallelogram (*prl*) configuration compared to the telescopic fork (solid blue). It can be observed that with both double wishbone suspension systems the head angle (ε) variation mostly follows that of the telescopic fork. Regarding to the normal trail (t_n), its behaviour with the Hossack system is similar to that
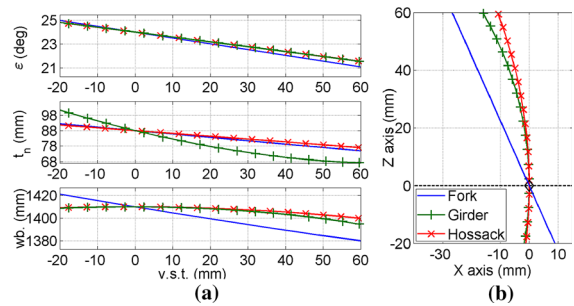

Fig. 8 Kinematic behaviour of the Girder (green plus) and Hossack (red cross) suspension systems with ***prl* configuration** compared with the telescopic fork (solid blue). The head angle (ε.), the normal trail (t_n) and the wheelbase (wb) variation with the vertical suspension travel (*v.s.t.*) are presented in (**a**). The trajectories of the front wheel's contact point along the full suspension travel are plotted in (**b**). (Color figure online)

with the telescopic fork, whilst the Girder suspension presents a more pronounced decrease of this parameter with the vertical suspension travel (*v.s.t.*). Finally the wheelbase (wb) behaves similarly with both Girder and Hossack suspension systems. This value is always reduced relative to the nominal position although in a less relevant manner, compared to the telescopic fork.

Figure 8b shows the trajectories of the front wheel contact points along the full suspension travel obtained with parallelogram configuration of the double wishbone suspension systems compared to that of the telescopic fork. Both Girder and Hossack systems produce curved trajectories. These trajectories are close to each other, have positive slopes between − 20 and + 10 mm of *v.s.t.* and differ from the nominal trajec-
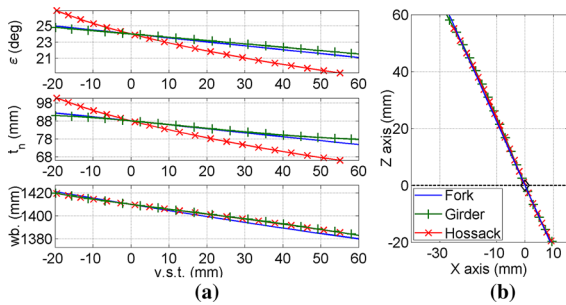
Fig. 9 Kinematic behaviour of the Girder (green plus) and Hossack (red cross) suspension systems with ***tft* configuration** compared with the telescopic fork (solid blue). The head angle (ε.), the normal trail (t_n) and the wheelbase (wb) variation with the vertical suspension travel (*v.s.t.*) are presented in (**a**). The trajectories of the front wheel's contact point along the full suspension travel are plotted in (**b**). (Color figure online)

Fig. 10 Kinematic behaviour of the Girder (green plus) and Hossack (red cross) suspension systems with ***cnt* configuration** compared with the telescopic fork (solid blue). The head angle (ε.), the normal trail (t_n) and the wheelbase (wb) variation with the vertical suspension travel (*v.s.t.*) are presented in (**a**). The trajectories of the front wheel's contact point along the full suspension travel are plotted in (**b**). (Color figure online)

tory returned by the telescopic fork, which has constant negative slope.

Similar plots are obtained for the Girder and Hossack suspension systems with telescopic fork's trajectory configuration (*tft*) in Fig. 9. The trajectories reached by both double wishbone suspension systems are almost identical to that of the telescopic fork (Fig. 9b). In the case of the Girder suspension system, the handling geometric parameters behave similarly to those with the telescopic fork suspension (Fig. 9a). This is the expected behaviour as the steering axis and the wheel trajectories are equal in both systems. However, for the Hossack suspension system, the steering axis varies with the suspension travel, which leads to different behaviours of the handling geometric parameters. The variation in the head angle and the normal trail with the vertical suspension travel are significantly larger for the Hossack system than for the telescopic fork suspension. However, the wheelbase is modified in a similar way, as the front wheel follows the same trajectory in both cases.

Being the normal trail a crucial parameter in the motorcycle handling, it could be an interesting feature for a suspension system to maintain this value constant at any position of the suspension travel. Kinematic behaviours of the Girder and Hossack suspension systems with a constant normal trail configuration (*cnt*) are represented in Fig. 10a. Almost constant normal trails are achieved by both Girder and Hossack suspension systems, with small deviations from their nominal values. As expected, in the case of the Girder suspension, the head angle maintains its nominal behaviour with the vertical suspension travel whilst the wheelbase is
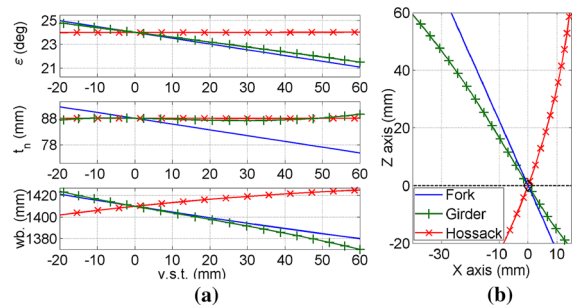
reduced. However, the Hossack suspension system with *cnt* configuration returns an almost constant head angle and, oppositely to the Girder and telescopic fork systems, the wheelbase is increased in compression and decreased in extension.

Regarding to the front wheel's contact point in Fig. 10b, it can be observed that with the Girder system, the trajectory is mostly a straight line at an angle with the vertical which is greater than that of the telescopic fork's trajectory. In the case of the Hossack system, the front wheel follows a curved trajectory. The angle with the vertical becomes negative in this case, reducing its value under compression and increasing it under extension. These trajectory angles will directly affect the suspension systems' anti-dive capabilities. Contrary to the behaviour of the telescopic fork system, both double wishbone suspension systems show a wide range of possible kinematic configurations. Either Hossack or Girder systems could be a good choice depending on the motorcycle's kinematics requirements.

4 Dynamical modelling

In order to study the dynamic properties of Girder and Hossack suspension systems, two mathematical models have been built using VehicleSim. Each of these models geometry has been modified with the design parameters values obtained in the previous section for the three kinematic configurations: parallelogram (*prl*), telescopic fork's trajectory (*tft*) and constant normal trail (*cnt*). Therefore, three different configurations of

each of the Girder and Hossack suspension systems are obtained.

The mathematical models here presented are developed as modifications of the Suzuki GSX-R1000 nominal model, derived in [23], which was built considering the actual physical properties of the original motorcycle's parts. The masses, the moments of inertia and the centres of masses were directly measured for each part. However, real GSX-R1000 motorcycles are not fitted with either Girder or Hossack suspensions. Therefore, the physical properties of these parts cannot be measured and included in the mathematical model. In order to obtain accurate values of these properties, a 3D computer-aided design (CAD) has been developed for each suspension system. The software used for this task was SolidWorks [3], which also allowed to perform the different compliance analyses (FEA) through its SolidWorks Simulation tool, needed to determine the designs consistency and reliability.

4.1 3D design and compliance analysis

It is important to note that this part of the research is not intended to obtain high performance commercial suspension systems, but to provide a good approximation of the mechanical parts of each suspension system under study. Therefore, the masses, the centres of mass, the inertia moments, etc., represent close values to those of a possible real suspension system implementation.

Both Girder and Hossack suspension systems are designed in order to keep the same front end assembly's mass as that of the original telescopic fork of the GSX-R1000 model. Each part's mass tends to be equal to the equivalent part in the telescopic fork case. However, due to the structural differences between the three suspension systems, this is not always possible. For instance, in the case of the Hossack suspension, the steering assembly consists only of a triple tree. This makes the Hossack systems much lighter than the telescopic fork system. The Girder suspension is only a few grams lighter than the telescopic fork. Nevertheless, in both Girder and Hossack cases the mass difference is added to the chassis body as a mass placed at the same coordinates as those of the steering body's centre of mass.

A construction material is associated to the different parts of the suspension systems, so that the dynamic properties of each part can be calculated. The mate-

rial chosen for both Girder and Hossack suspension systems was 7075 aluminium alloy, commonly used in automotive industry due to its light weight and strength. The suspension systems have been designed in order to support the maximum loads that appear during extreme running conditions, such as extreme braking or high speed and high lean angle manoeuvres. Various finite element analyses were carried out for each suspension system in order to ensure their integrity and reliable performance under those heavy loads. A factor of safety greater than two is found for all the simulations, even though the assemblies masses are smaller than the conventional telescopic fork and the loads applied were increased in simulation an extra 50% over the theoretical maximum loads calculated. Figure 11 shows the FEA results for maximum lateral load, maximum longitudinal load for extended suspension and maximum longitudinal load for compressed suspension. Although more detailed studies would be needed, these results suggest that even lighter designs could be obtained for these kinds of suspension. Despite that is not the objective of this research, these results allow to be confident in the dynamic properties computed for the parts of the different assemblies, being close to those properties of eventual realistic designs of these suspension systems.

In order to obtain a coherent comparison between the three different suspension systems, they have been divided in four subsystems each of them containing different parts. The parts belonging to each subsystem depend on which suspension system is considered.
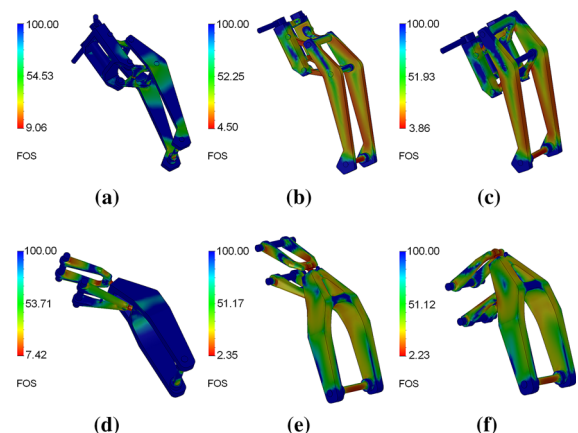

Fig. 11 Factor of safety computed by FEA for the Girder (top row) and Hossack (bottom row) models under maximum lateral load (**a**, **d**), maximum longitudinal load for extended suspension (**b**, **e**) and maximum longitudinal load for compressed suspension (**c**, **f**)

Table 4 Masses for the bodies of the different suspension systems models

Mass (kg)	STR	SUS	UWB	LWB	Total
Fork	9.990	7.250	–	–	17.240
Girder	7.863	7.930	0.666	0.764	17.223
Hossack	1.1692	7.1489	0.976	0.924	10.218

STR It is the body that allows the steering action. It comprises the triple trees and eventually other parts depending on the model under consideration. In the case of the telescopic fork it also includes the upper tubes. In the case of the Girder, the mass of the upper part of the spring-damper unit is also included. In the case of the Hossack system, it includes the upper lever of the steering linkage.

SUS It represents the body holding the front wheel. In the case of the telescopic fork it comprises the lower tubes of the fork. In the case of the Girder and Hossack suspension systems, this body corresponds to the uprights, the lower part of the spring-damper unit and, only for the Hossack system, the lower lever of the steering linkage.

UWB This part is exclusively defined for the Girder and Hossack systems. It only consists of the upper wishbone.

LWB This part is exclusively defined for the Girder and Hossack systems. It only consists of the lower wishbone.

The dynamic properties of each subsystem can be obtained from the 3D model in SolidWorks. Table 4 shows the masses of each part on the different suspension systems compared to the original telescopic fork parts masses. In the case of the Hossack system, the remaining mass needed to equal that of the original telescopic fork is 7.022 kg. However, as it has been said, an equivalent mass is added to the chassis body in the same coordinates than those of the steering body's centre of mass maintaining the overall motorcycle mass for both suspension systems.

4.2 Mathematical modelling

The GSX-R1000 model presented in Sect. 2 has been modified to include multi-body representations for both the Girder and the Hossack suspension systems. In both cases, and similarly to the original nominal model, a massless body is included (the twist body) to repre-

sent the frame's flexibility. The flexibility is defined as a rotational degree of freedom between the motorcycle chassis (rear frame) and the front suspension (front frame) about the twist axis. This is an axis perpendicular to the steering one which lies within the motorcycle's symmetry plane and passes through the attachment point of the twist body. This point is defined in both suspension systems as the middle point between the upper and the lower wishbones joint coordinates (points q_1 and q_2 in Fig. 5). For each of the suspension models, a different parent–child relation between the different bodies is implemented.

The parent–child structure of the Girder suspension is shown in Fig. 12. The steer body is attached to the twist body, allowing the rotation about its z axis. The twist's body reference frame shares its y axis with the main frame's y axis. The twist body's reference frame is rotated about the y axis making coincident its x axis with the twist axis in the main frame. All the bodies after the twist body have a similar reference frame orientation. Therefore, the z axes of the twist and the steer bodies are parallel with the steering axis in the main body reference frame. The mass, the moments of inertia and the inertia products of this body correspond to those of the Girder's STR subsystem stated in the previous section. The rider's steering moment and the steering damper moment are applied to the steer body about
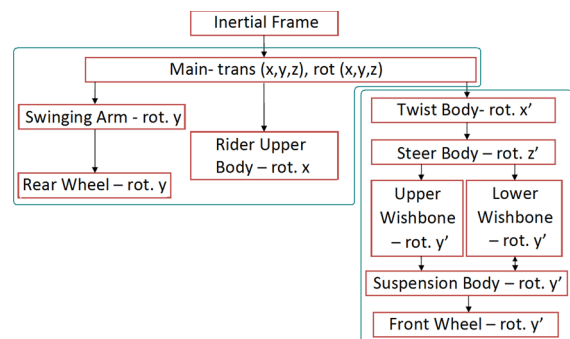

Fig. 12 Parent–child structure of the motorcycle model modified with the Girder suspension system

its z axis and react on the rider's upper body and on the main body, respectively. The upper wishbone and lower wishbone bodies are children of the steer body and both rotate about the y axis. Their masses and their moments and products of inertia are obtained from the CAD designs and correspond to the Girder's UWB and LWB subsystems, respectively. The suspension body is a child of the upper wishbone body. It also rotates about the y axis (only) and its mass, moments and products of inertia correspond to those of the Girder's SUS subsystem. The closure of the kinematic loop is done between the lower wishbone and the suspension body. The geometrical point of the lower wishbone's tip is defined as coincident with the wishbone attachment point in the suspension body (point q_3 in Fig. 5a) by position constraints in x, y and z directions. The rotational degrees of freedom about axes x and z are also removed. Therefore, the only motion allowed between the lower wishbone and the suspension body is the rotation about their common y axis. Finally, the suspension body is the parent of the front wheel body, which has same properties and kinematics as the original GSX-R1000 nominal model, rotating about its y axis.

Following the different mechanical configuration of the Hossack suspension system, in which the steering axis is placed on the four-bar linkage's opposite side, a different parent–child structure must now be considered. This is shown in Fig. 13. In this case, the two wishbones are connected directly to the twist body and rotate about their y axis corresponding to that of the twist body. Their mass and inertia properties were found previously as those of the Hossack's UWB and LWB subsystems. The suspension body is a child of the upper wishbone body. Its mass, inertia moments and inertia products correspond to the Hossack SUS subsystem. In the Hossack model, the suspension body also performs the system's steering action. Thus, in its joint with the upper wishbone, the suspension body is allowed to rotate about the common y axis and its own z axis. The kinematic loop closure in this case, as in the Girder suspension, is done between the lower wishbone and the suspension body. The geometrical point of the lower wishbone's tip is defined as coincident with the lower wishbone attachment point in the suspension body (point q_3 in Fig. 5b) by position constraints in x, y and z directions. However, in this case, in addition to the common y axis rotation allowed between the lower wishbone and suspension body in the Girder suspension case, rotation about the suspension body z axis is
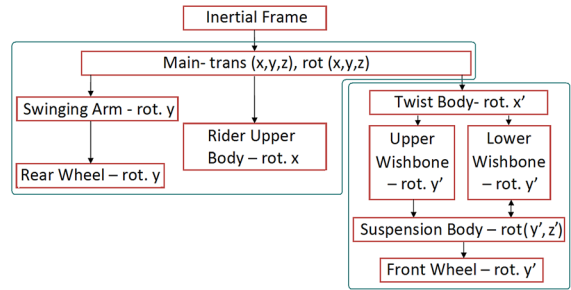

Fig. 13 Parent–child structure of the motorcycle model modified with the Hossack suspension system

also allowed between the lower wishbone and suspension body. Finally, the front wheel body is connected to the suspension body and rotates about its y axis. It has a similar definition to that in the telescopic fork and the Girder suspension models. Considering that the inertia moment and products obtained for the Hossack STR subsystem are negligible and that it does not play a significant role on the front end kinematics, its mass is directly lumped into the main body's mass, whose centre of masses is modified according to the relative position of this subsystem. In the Hossack suspension system, the rider's steering and the steering damper moments are directly applied to the suspension body about its z axis. The first reacts on the rider's upper body whilst the second does so on the main body.

4.3 Suspension tuning

The suspension forces in both Girder and Hossack systems are modelled as two moments applied to the lower wishbones and reacting on the steer body and the twist body, respectively. These suspension moments depend on the lower wishbones angular displacements and speeds, providing the reactive and the dissipative suspension actions. This work is focused on comparing the two alternative suspension systems performance to that of the telescopic fork system. Thus, in order to introduce the minimum systems variations, it is sought a stiffness/damping tuning, for both Girder and Hossack systems, equivalent to that of the telescopic fork suspension. Following the approach in [2], the equivalent suspension moments to the linear suspension force of the telescopic fork can be calculated considering an energy conservation condition: the sum of the energy stored and dissipated by the torsional

spring and damper, respectively, in the double wishbone system is equivalent to that of the linear spring and damper in the telescopic fork, for the same vertical displacement of the front wheel attachment point and in the same time. Finally, the stiffness moment and the damping coefficient are described through third-order polynomial fits on the angle rotated by the lower wishbone. The damping moment results from multiply the damping coefficient and the angular rate. The maximum error achieved by this approximation is less than 2% along the full suspension travel.

5 Suspension response

The responses of the different suspensions systems are tested and compared to the conventional telescopic fork response under two different running situation. The first considers the motorcycle passing straight through a step bump input. In the second one, the motorcycle performs a hard front braking manoeuvre. Several simulations are carried out in both cases for different motorcycle forward speeds. The results are found to be qualitatively similar for the different forward speeds under study. In here, the simulations at 40 m/s are taken as example to illustrate these results.

5.1 Road bump input

The road bump input simulation is performed with the motorcycle running in straight line. After a few metres, a step input of height $h_b = 50$ mm is applied. This step bump is computed taking into account both vertical and horizontal forces appearing on the tyres when they reach the bump corner.

Figure 14 compares the front end responses to a bump input of the motorcycle fitted with a telescopic fork and with Girder and a Hossack suspension systems designed with a parallelogram (*prl*) configuration. In Fig. 14a the vertical displacement of the motorcycle handle bar is presented whilst Fig. 14b presents the vertical displacement of the front wheel centre. Although the overshoot is slightly higher for both Girder and Hossack suspension systems, it can be appreciated that the behaviours of the three models are very similar.

When both suspension systems are designed with a fork's trajectory (*tft*) configuration, the Girder system shows a response almost identical to the telescopic fork
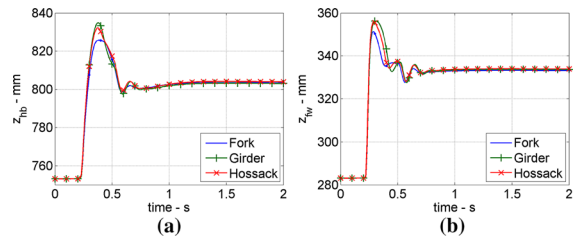

Fig. 14 Motorcycle front end response after a 50 mm road bump input with a forward speed of $v = 40$ m/s for the **parallelogram configuration** (*prl*) of both Girder and Hossack suspension systems. **a** Handlebar height, **b** front wheel height
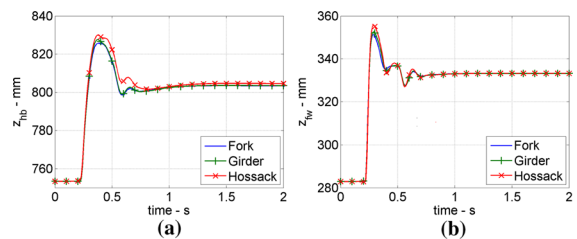

Fig. 15 Motorcycle front end response after a 50 mm road bump input with a forward speed of $v = 40$ m/s for the **telescopic fork's trajectory configuration** (*tft*) of both Girder and Hossack suspension systems. **a** Handlebar height, **b** front wheel height

suspension case. It is the Hossack suspension system which introduces small behaviour differences. These results, shown in Fig. 15, are coherent with the fact that the steering axle in the Girder and the fork suspension systems is fixed to the chassis, and in both cases, the front wheel follows the same trajectory. Consequently, the motions of the masses in both fork and Girder systems are close.

Figure 16 shows the results for the road bump input simulation for the two alternative suspension systems designed in order to introduce a minimal normal trail variation (*cnt* configuration). Whilst the Hossack system response slightly differs, the Girder suspension response is closer to that of the telescopic fork.

Both alternative suspension systems have been designed to obtain similar stiffness and damping properties to the telescopic fork. However, the different mechanical configurations and mass distribution of these systems introduce small variation in the motorcycle front end response. Although a more precise tuning of each alternative suspension system would result in more efficient response of the front end, it can be said that different kinematics configurations(*prl*, *tft* and *cnt*)
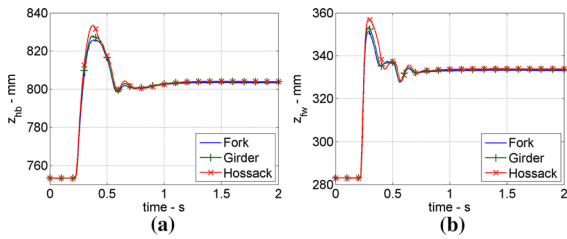
Fig. 16 Motorcycle front end response after a 50 mm road bump input with a forward speed of $v = 40$ m/s for the **constant normal trail configuration** (*cnt*) of both Girder and Hossack suspension systems. **a** Handlebar height, **b** front wheel height

do not introduce significant variation in the suspension performance.

5.2 Front wheel braking

Front wheel braking manoeuvres are simulated for a constant deceleration of $a = -0.5$ G. As it has been explained in Sect. 2, a PD controller implemented in the model calculates the braking moment to be applied to the front wheel in order to obtain the desired deceleration. In order to focus on the pure braking effects only, the aerodynamic forces have not been taken into account by setting the drag, lift and pitch aerodynamic coefficients to zero during this simulations. The diving of the motorcycle's front end and the variation in normal trail are compared between the double wishbone suspension systems and the telescopic fork suspension.

Figure 17 shows the vertical suspension travel and the normal trail variation of the three different motorcycle models fitted with the telescopic fork, the Girder and the Hossack suspension systems with a parallelogram configuration (*prl*). The anti-dive effect is shown to increase in Fig. 17a for both double wishbone suspension systems. This is produced by their front wheels contact points trajectories which can be observed in Fig. 8. However, regarding to the normal trail variation, the Girder and Hossack systems behave opposite to each other. Whilst the Girder suspension reaches smaller normal trail values than the telescopic fork, the Hossack system presents larger normal trail values than the fork for all the suspension travel.

When both Girder and Hossack suspension systems are designed with a fork's trajectory configuration (*tft*), their diving properties become similar to those of the telescopic fork, as it is shown in Fig. 18. The vertical suspension travel reached under the braking manoeuvre
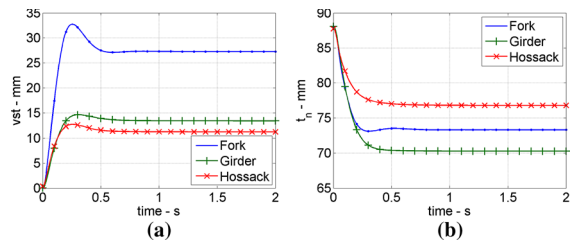

Fig. 17 Vertical suspension travel (*v.s.t.*) and normal trail (t_n) for the telescopic fork suspension compared to the Girder and Hossack systems with a **parallelogram configuration** (*prl*). A straight line front wheel braking manoeuvre at an initial forward speed of $v = 40$ m/s with a constant deceleration of $a = -4.9$ m/s^2 is performed. **a** Vertical suspension travel, **b** normal trail
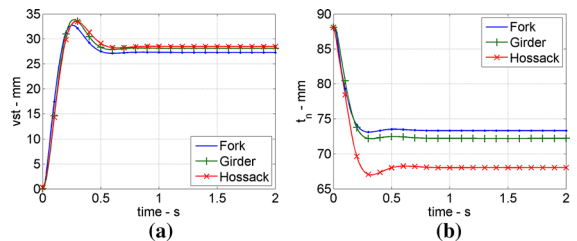

Fig. 18 Vertical suspension travel (*v.s.t.*) and normal trail (t_n) for the telescopic fork suspension compared to the Girder and Hossack systems with a **telescopic fork's trajectory configuration** (*tft*). A straight line front wheel braking manoeuvre at an initial forward speed of $v = 40$ m/s with a constant deceleration of $a = -4.9$ m/s^2 is performed. **a** Vertical suspension travel, **b** normal trail

is similar for the three systems. In the Girder suspension and telescopic fork cases, the common steering axles and front wheel contact points trajectories produce similar kinematics in both systems, which results in similar normal trail behaviour.

In the Hossack suspension system case, the normal trail is highly reduced from $t_n = 88$ mm up to $t_n = 68$ mm, which exceeds significantly the reduction of this parameter reached by the telescopic fork and Girder suspension systems. The Hossack system's geometry magnifies the normal trail reduction. In order to obtain a front wheel contact point trajectory similar to that of the telescopic fork, the steering angle is necessarily reduced with the suspension travel. This leads to a greater normal trail reduction compared to other configurations.

Figure 19 shows the front end behaviour of the Girder and the Hossack systems configured to present a minimal normal trail variation under a front wheel
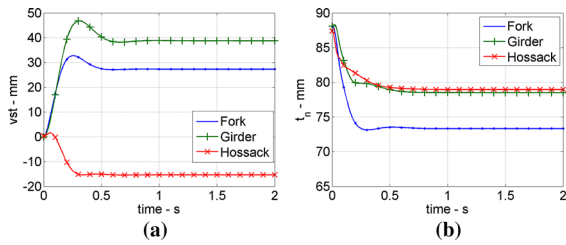
Fig. 19 Vertical suspension travel (*v.s.t.*) and normal trail (t_n) for the telescopic fork suspension compared to the Girder and Hossack systems with a **constant normal trail configuration** (*cnt*). A straight line front wheel braking manoeuvre at an initial forward speed of $v = 40$ m/s with a constant deceleration of $a = -4.9$ m/s^2 is performed. **a** Vertical suspension travel, **b** normal trail

braking manoeuvre. The front wheel contact point trajectory becomes highly relevant on the suspension's anti-dive effect. Looking at Fig. 10b it can be observed a trajectory of the contact point with a larger angle with the vertical that the Girder suspension produces, which makes this configuration of the Girder suspension system more prone to dive than the telescopic fork. This results in an increase of the vertical suspension travel about 10 mm with respect to the telescopic fork system.

Conversely, the Hossack suspension system with this configuration shows a negative angle of its front wheel contact point trajectory with the vertical. This results in an opposite behaviour of the front end, which rises from its nominal position about 15 mm. Regarding to the normal trail, both Girder and Hossack suspension systems experience a reduction (limited by the geometrical configuration) of this value, as shown in Fig. 19b. Even though they were both designed to keep this value constant, this can only be achieved by considering the static suspension compression. Depending on the different accelerations on the motorcycle, other elastic parts different than those of the front suspension system will be compressed or extended: these are the tyres carcasses and the swinging arm assembly. This geometry variation changes the kinematics design and produces a normal trail reduction; however, this reduction is not as large as for the telescopic forks suspension.

Whilst the kinematics of the front suspension systems do not affect in a significant manner the suspension response to a bump, it does affect the anti-dive effect and the motorcycle geometry variation under braking manoeuvres. Depending on the specifications sought, different systems may be adopted. For instance,

if higher values of anti-dive and a reduction of normal trail under braking are required, then a Girder suspension systems would provide a good kinematic solution. On the other hand, for a reduced variation of the normal trail avoiding the diving of the motorcycle whilst braking, a Hossack system can be used.

6 Stability analysis

In order to understand how the double wishbone suspension systems may affect the motorcycle oscillatory dynamics, stability analyses are performed taking advantage of root loci of the different linearized motorcycle models. The stability of both double wishbone suspension systems is studied for various parameter variations such as geometry configuration, front frame compliance and steering damper coefficients. Following the approach stated in Sect. 2, the state space models derived from the linearized equations of motion are fed with the quasi-equilibrium states, integrated from the nonlinear equations. These states have been obtained for each model, from four motorcycle simulations with four different roll angles (0°, 15°, 30° and 45°). In each simulation, the forward speed is increased from 10 m/s up to 80 m/s with an acceleration of $a = 0.001$ m/s^2.

Figure 20 shows these root loci of the nominal motorcycle model fitted with a telescopic front fork. The rider lean, weave and wobble oscillating modes are shown. Also the pitch mode appears in the area of interest, but only for the case of a 45° roll angle. The rest of the normal modes are highly damped and are not visible in this area.
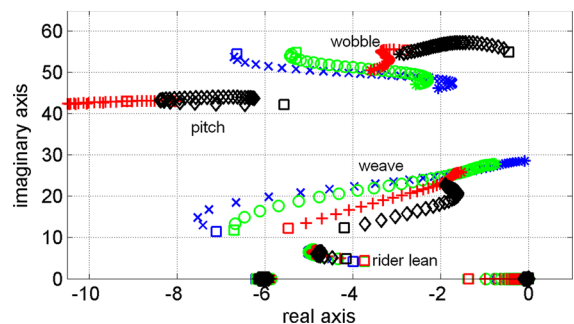

Fig. 20 Root loci of the nominal motorcycle model fitted with a telescopic fork suspension. The speed is increased from 10 m/s (open square) up to 80 m/s (asterisk) at different roll angles: 0° (blue cross), 15° (green open circle), 30° (red plus) and 45° (black open diamond). (Color figure online)

Under straight running conditions, the rider lean, weave and wobble are out-of-plane modes whilst the pitch mode is an in-plane one. When cornering, the in-plane and out-of plane variables become coupled. The pitch mode consists in the pitching of the motorcycle through the front and rear suspension compression and extension in an almost phase opposition motion. The rider lean appears in the root locus when the rider upper-body degree of freedom is included in the mathematical model. It represents the oscillation of the rider's upper body. The weave mode involves roll, yaw and steering angle oscillations combined in a fishtailing motion. The wobble mode is characterized by a shaking of the front frame about the steering axis whilst the rear frame is slightly affected. The in-plane and the out-of-plane degrees of freedom become coupled for roll angles different to zero, when the motorcycle symmetry plane is no longer vertical. Weave and wobble oscillating modes have been widely studied in the literature (e.g. [1,6,11,12,17,20] just to cite a few) and they are of main relevance in this research due to their lightly-damped nature and the possibility to become unstable under some running conditions.

6.1 Geometry variation

Fitting a different suspension system may affect the motorcycle stability. However, for each suspension system under study, its geometrical configuration (*prl*, *tft* and *cnt*) does not modify in a significant manner the system's roots positions of the motorcycle fitted with that suspension.

As an example, Fig. 21a, b shows the root loci for four different simulations at various motorcycle's lean angles for the Girder suspension with the telescopic fork's trajectory (*tft*) and the constant normal trail (*cnt*) configurations.

Compared to the root loci for the telescopic fork suspension (Fig. 20), three things can be observed: first, the destabilization of the weave mode at zero roll angle for speeds above 70 m/s. At higher roll angles (15°, 30° and 45°), this mode is less damped than in the telescopic fork suspension case but does not cross the stability limit. Secondly, the wobble mode is unstable for speeds lower than 16 m/s at 45°. However, it becomes more damped for higher speeds and smaller roll angles. Finally, the third effect of fitting the motorcycle with such a Girder suspension system is an appre-
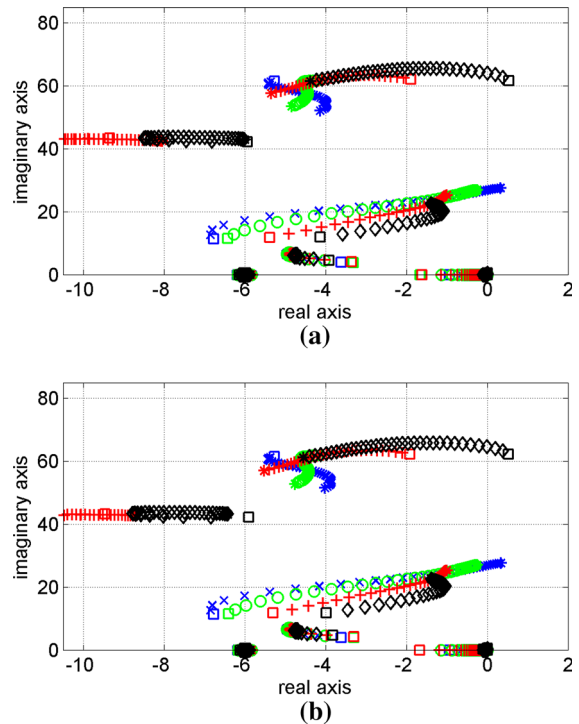

Fig. 21 Root loci for the Girder suspension with telescopic fork's trajectory (*tft*) and constant normal trail (*cnt*) configurations. The speed is increased from 10 m/s (open square) up to 80 m/s (asterisk) at different roll angles: 0° (blue cross), 15° (green open circle), 30° (red plus) and 45° (black open diamond). **a** Girder—*tft* config, **b** Girder—*cnt* config. (Color figure online)

ciable increase of the wobble frequency. The rest of the modes remain mostly unaffected by the inclusion of this suspension system on the motorcycle model.

On the other hand, the geometrical configuration of the Hossack system does not introduce relevant differences on the system's roots. As an example Fig. 22a, b shows the root loci for four lean angles simulations of the Hossack suspension system with the parallelogram (*prl*) and the constant normal trail (*cnt*) configurations, respectively.

Compared to the root loci of the telescopic fork suspension case, the Hossack suspension system's wobble mode becomes more damped at higher forward speeds for all roll angles whilst it is less damped at lower speeds. In the case of 45° roll angle, this mode is unstable below 20 m/s. The remaining normal modes are not substantially affected by the inclusion of this suspension system in the motorcycle model.
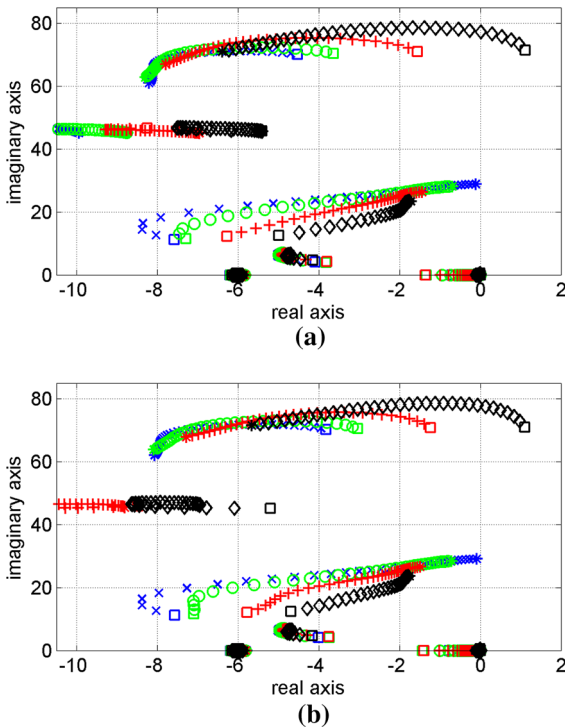
Fig. 22 Root loci for the Hossack suspension system with parallelogram (*prl*) and constant normal trail (*cnt*) configurations. The speed is increased from 10 m/s (open square) up to 80 m/s (asterisk) at different roll angles: 0° (blue cross), 15° (green open circle), 30° (red plus) and 45° (black open diamond). **a** Hossack—*prl* config, **b** Hossack—*cnt* config. (Color figure online)

Fig. 23 Root loci for the Girder suspension system with constant normal trail (*cnt*) configuration. The twist moment coefficients are varied as 60% (blue cross), 80% (green open circle), 100% (magenta dot), 120% (red plus) and 140% (black open diamond) of the nominal value. The speed is increased from 10 m/s (open square) up to 80 m/s (asterisk) at different roll angles. **a** Girder—roll = 0° (twist moment variation), **b** Girder—roll = 45° (twist moment variation). (Color figure online)

6.2 Front frame compliance

The design of a front suspension system will determine its compliance and, hence, the stiffness at the front end. It is interesting to study how this compliance can affect the stability of a motorcycle assembly. In the GSX-R1000 nominal mathematical model, the compliance is introduced as a reacting moment applied between the chassis and the front end about the twist axis which is an axis perpendicular to the steering one and belonging to the motorcycle symmetry plane.

The twist moment was defined as a torsional spring and damper combination whose stiffness and damping parameter nominal value was set to $k_{t0} = 100$ kNm and $c_{t0} = 100$ Nms. In order to study the variation on the rigidity of both front suspension systems, these stiffness and damping coefficients are modified proportionally from 60% of their nominal values up to the 140%. These maximum values may be difficult to be achieved in a real mechanical implementation, but
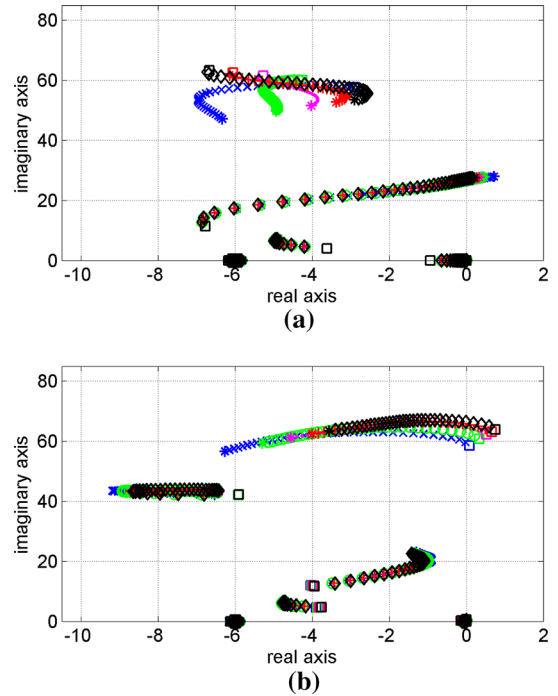
become useful to be considered in order to highlight the trends of the system's behaviour.

As it has been shown, since the variation in the geometrical configuration of both Girder and Hossack suspension systems does not affect their stability properties significantly, Figs. 23 and 24 show the root loci of the Girder and Hossack systems for the different values of the twist moments only for the constant trail geometrical configuration (*cnt*). On the other hand, considering that the more relevant stability issues appear for roll angles of 0° and 45°, the root loci for 15° and 30° are not presented in order to obtain clearer results. Therefore, the root loci are plot for an unique roll angle, with different stiffness and damping coefficients values and with the speed varied from 10 m/s up to 80 m/s.

For the Girder suspension system with nominal values of twist moment coefficients, the weave mode is unstable for speeds above 70 m/s at a zero roll angle, whilst the wobble mode instability happens for a 45°
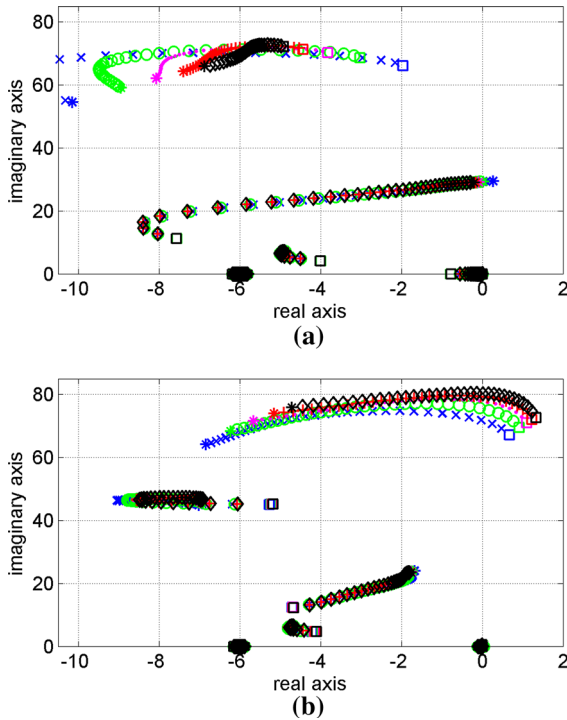
Fig. 24 Root loci for the Hossack suspension system with constant normal trail (*cnt*) configuration. The twist moment coefficients are varied as 60% (blue cross), 80% (green open circle), 100% (magenta dot), 120% (red plus) and 140% (black open diamond) of the nominal value. The speed is increased from 10 m/s (square) up to 80 m/s (asterisk) at different roll angles. **a** Hossack—roll = 0° (twist moment variation), **b** Hossack—roll = 45° (twist moment variation). (Color figure online)

Fig. 25 Root loci for the telescopic fork suspension system. The twist moment coefficients are varied as 60% (blue cross), 80% (green open circle), 100% (magenta dot), 120% (red plus) and 140% (black open diamond) of the nominal value. The speed is increased from 10 m/s (square) up to 80 m/s (asterisk) at different roll angles. **a** Fork—roll = 0° (twist moment variation), **b** Fork—roll = 45° (twist moment variation). (Color figure online)

roll angle and forward speed values below 16 m/s. When the twist rigidity is increased, the wobble mode becomes more unstable whilst the weave mode's stability increases, narrowing in this way its unstable forward speed range at zero roll angle. A reduction of the twist rigidity results in the opposite effect. Consequently, weave and wobble modes' stability cannot be satisfied simultaneously by modifying the front suspension system's compliance.

Considering the Hossack suspension system, the front end's compliance variation has an impact on the motorcycle's stability behaviour similar to that in the case of the Girder suspension. In this case, the wobble mode at 45° roll angle is stable for speed values larger than 20 m/s whilst the weave mode is stable for practically all the speed range at any roll angle for the nominal value of the twist moment coefficient. However, if the stabilization of the wobble mode for a 45° roll angle at
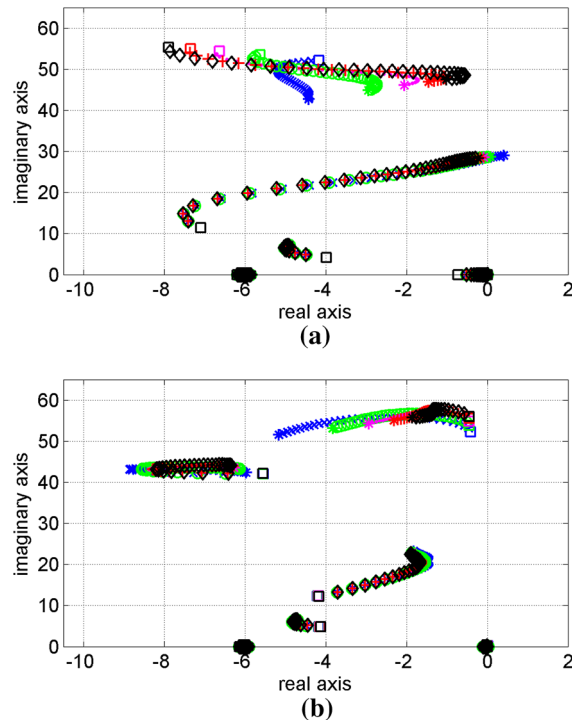
the lower speed range is sought by decreasing the front frame's rigidity, the weave mode will become unstable for the straight line case at its higher speed range.

If theses results are compared to a similar study for the telescopic fork (see Fig. 25), it can be observed that the effect of modifying the front end's compliance on the motorcycle general stability is similar for the three suspension systems: A positive increment of the twist bending moment increases the weave mode's stability and decreases the wobble mode's stability. On the other hand, by reducing the twist bending moment the weave mode become less stable whilst the wobble mode stability is increased.

6.3 Steering damper coefficient

The steering damper is a passive device which links the steering body and the chassis, whose mission is to attenuate wobble oscillations. Nowadays, a steering
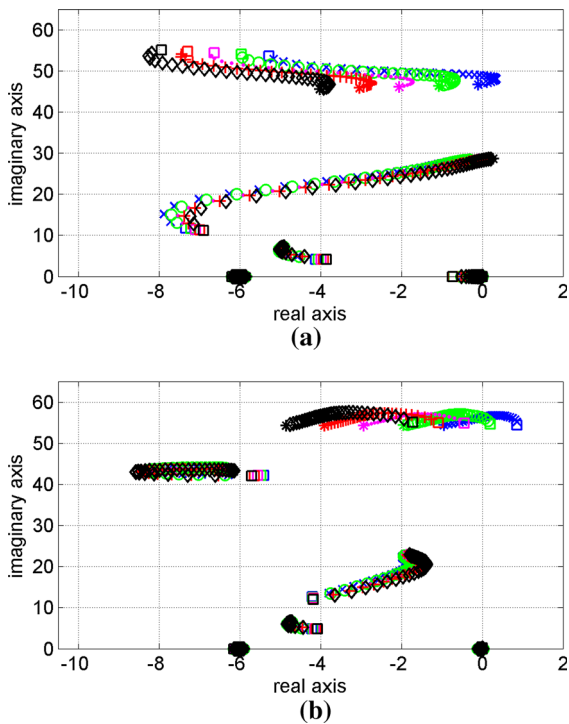
Fig. 26 Root loci for the telescopic fork suspension system. The steering damper coefficient is varied as 60% (blue cross), 80% (green open circle), 100% (magenta dot), 120% (red plus) and 140% (black open diamond) of the nominal value. The speed is increased from 10 m/s (open square) up to 80 m/s (asterisk) at different roll angles. **a** Fork—roll = 0° (steering damper variation), **b** Fork—roll = 45° (steering damper variation). (Color figure online)

Fig. 27 Root loci for the Girder suspension system with constant normal trail (*cnt*) configuration. The steering damper coefficient is varied as 60% (blue cross), 80% (green open circle), 100% (magenta dot), 120% (red plus) and 140% (black open diamond) of the nominal value. The speed is increased from 10 m/s (open square) up to 80 m/s (asterisk) at different roll angles. **a** Girder—roll = 0° (steering damper variation), **b** Girder—roll = 45° (steering damper variation). (Color figure online)

damper is fitted in most of the commercial sport motorcycles. The nominal GSX-R1000 model has a steering damper which is mathematically modelled as a linear reacting moment between the steering body and the motorcycle's main body (chassis).

Figures 26, 27 and 28 show the root loci of the motorcycle system fitted with telescopic fork, Girder and Hossack suspension systems for several simulations in which the steering damper coefficient was varied from the 60% of its nominal value ($c_{sd0} = 6.94$ Nms) up to the 140%. For the three suspension systems the results are similar. It is well known [7,8] that in the case of telescopic fork suspension systems, by increasing the steering damper coefficient the wobble mode becomes more stable, however, the weave mode stability at high forward speeds is compromised by the action of the steering damper. On the other hand, when the steering damping coefficient is reduced the effect on the motor-
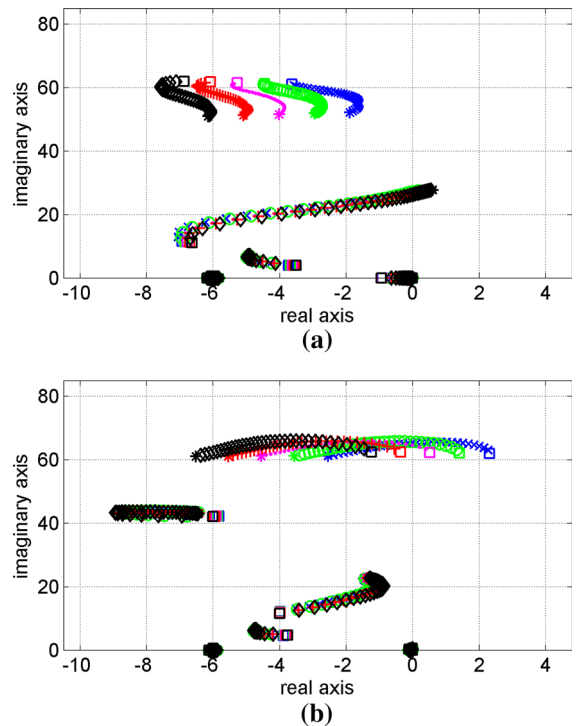
cycle stability is inverted. Girder and Hossack systems follow the same trend in terms of stability when the damping coefficient is varied, which is to be expected.

In the case of the Girder suspension, the weave mode stability is always compromised at high speeds ranges even for the smallest value of the steering damper coefficient. In this case, the wobble mode is unstable for half of the speed range at 45° roll angle. Stability of both modes cannot be achieved simultaneously with the steering damper. However, as a compromise solution, it can be used to stabilize the wobble mode at lower speed and high roll angles by sacrificing the weave stability at higher forward speed values.

It was found that for the GSX-R1000 model fitted with Girder suspension system with a constant normal trail configuration, the wobble mode becomes fully stable for a value of the steering damper coefficient of $c_{sd} = 7.85$ Ns, which is a 13% higher than the
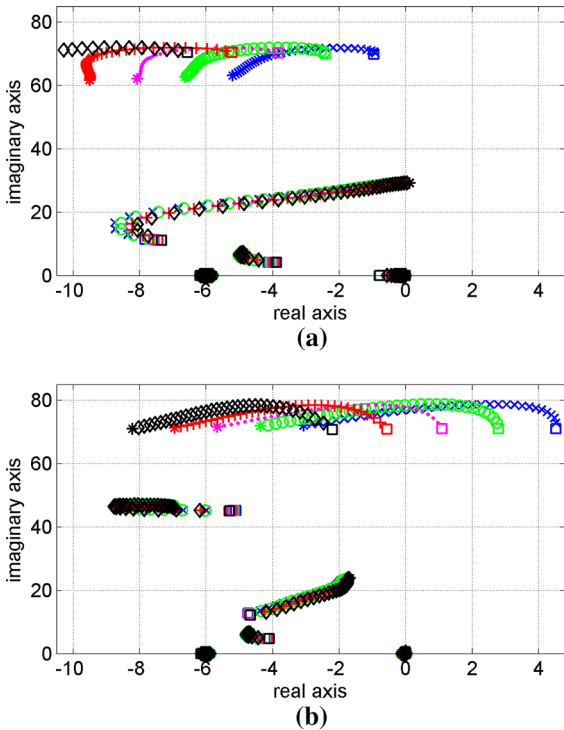
(a)

(b)

Fig. 28 Root loci for the Hossack suspension system with constant normal trail (*cnt*) configuration. The steering damper coefficient is varied as 60% (blue cross), 80% (green open circle), 100% (magenta dot), 120% (red plus) and 140% (black open diamond) of the nominal value. The speed is increased from 10 m/s (open square) up to 80 m/s (asterisk) at different roll angles. **a** Hossack—roll $= 0°$ (steering damper variation), **b** Hossack—roll $= 45°$ (steering damper variation). (Color figure online)

(a)

(b)

Fig. 29 Root loci for the Girder suspension system in which its centre of mass is displaced towards the steering axis. 68 mm forward (blue cross), 34 mm forward (green open circle), 0 mm (magenta dot) $-$ 34 mm backwards (red plus) and $-$ 68 mm backwards (black open diamond). **a** Girder—roll $= 0°$ (CM variation), **b** Girder—roll $= 45°$ (CM variation). (Color figure online)

nominal value. The maximum forward speed at which the weave mode still remains stable is $v = 70$ m/s, which for non-racing conditions is a considerable speed (252 km/h) above the legal speed limits. On the other hand, with a Hossack suspension system, the weave mode is better damped. A steering damper coefficient value which keeps both modes stable for almost all the studied running conditions can be found for the GSX-R1000 model fitted with this suspension system. This value is $c_{sd} = 7.92$ Ns, which is a 14% higher than the nominal value.

6.4 Location of the front frame's centre of mass

Due to the different designs of the three suspension systems, their centres of mass are differently located, as it is shown in Fig. 1. For the telescopic fork and
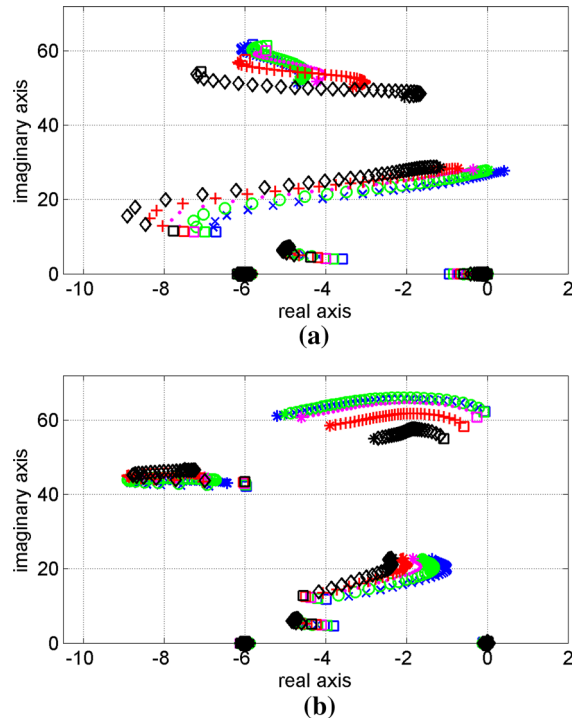
the Hossack suspension, their centres of mass are next to the steering axis. However, in the case of the girder suspension its centre of mass is placed about 68 mm ahead its steering axis.

This study was made by modifying the coordinates of the centres of mass of the SUS and STR parts in the different suspension systems in order to obtain the desired assembly's centre of mass. Figure 29 presents the impact on the root loci of displacing the centre of mass of the Girder suspension system. The distance of this point to the steering axis takes the following values: 68 mm forward (blue ×), 34 mm forward (green ○), laying on the steering axis (magenta ·), $-$ 34 mm backwards (red +) and $-$ 68 mm backwards (black ◊). Similar studies are performed for the Hossack and the telescopic fork suspension systems. Figures 30 and 31 show these results.

For the three suspension systems, it is found that, by displacing the centre of mass towards the steering axis
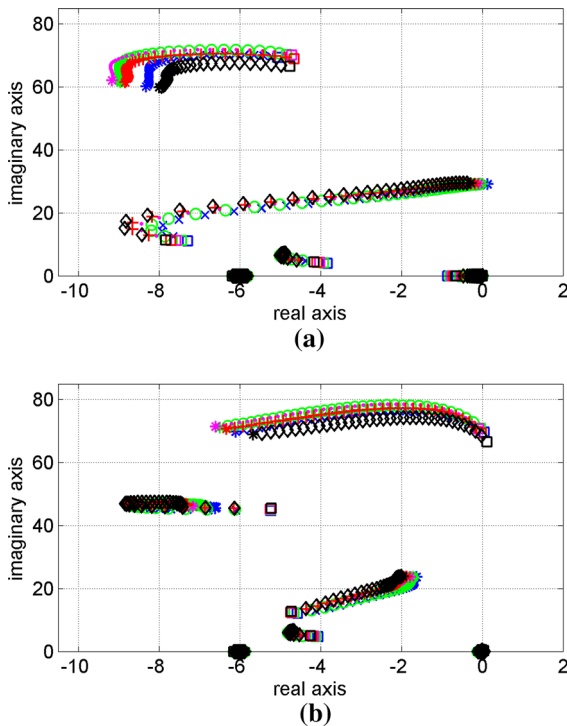
Fig. 30 Root loci for the Hossack suspension system in which its centre of mass is displaced towards the steering axis. 68 mm forward (blue cross), 34 mm forward (green open circle), 0 mm (magenta dot) − 34 mm backwards (red plus) and − 68 mm backwards (black open diamond). **a** Hossack—roll = 0° (CM variation), **b** Hossack—roll = 45° (CM variation). (Color figure online)

Fig. 31 Root loci for the telescopic fork suspension system in which its centre of mass is displaced towards the steering axis. 68 mm forward (blue cross), 34 mm forward (green open circle), 0 mm (magenta dot) − 34 mm backwards (red plus) and − 68 mm backwards (black open diamond). **a** Fork—roll = 0° (CM variation), **b** Fork—roll = 45° (CM variation). (Color figure online)

from its nominal position, the stability of weave and wobble modes is significantly increased. The stability of the weave mode is always improved by displacing backwards the centre of mass. The wobble mode becomes more stable when the centre of mass is close to the steering axis. However, if it is displaced backwards over a certain limit, the wobble mode starts to approach instability.

In both Girder and Hossack suspension system, when the centre of mass is laying on the steering axis, the weave and wobble normal modes become stable even with the nominal value of the steering damper. These results suggest that whilst a Hossack suspension system can be designed as a fully stable system just by tuning the steering damper, a Girder suspension system will present stability issues due to its geometry and mass distribution.
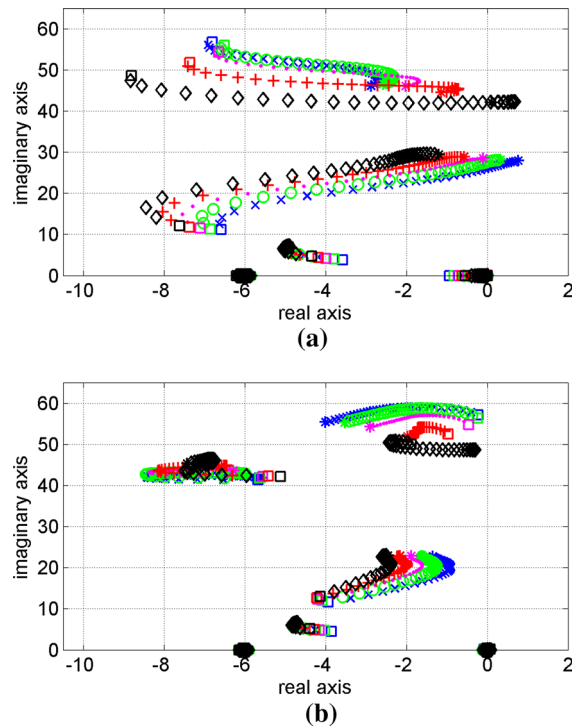
7 Conclusions

The main goal of this research is to understand how the different geometrical configurations of double wishbone suspension systems may affect the motorcycle dynamics and stability. The dynamic response and the stability properties of an existing motorcycle model modified with different geometrical configurations of two representative double wishbone suspension systems (Girder and Hossack) have been investigated and compared to those of the baseline model fitted with a telescopic fork suspension.

Several simulations were performed to test the dynamical response of the double wishbone suspension systems. For front wheel braking manoeuvres, the designs of the different suspension systems become crucial for their responses. The anti-dive capabilities of double wishbone suspension systems depend directly on the front wheel trajectory that they can

perform. For the nominal parallelogram configuration (*prl*), both Girder and Hossack suspension systems have similar responses providing some anti-dive compared to the telescopic fork. However, when both Girder and Hossack suspension systems are designed with the telescopic fork trajectory configuration (*tft*), their behaviour is similar to that of the telescopic fork and does not provide extra anti-dive. Finally, when constant normal trail configuration (*cnt*) is implemented, the kinematic differences in the two double wishbones suspensions designs imply different behaviours. Whilst Girder suspension dives further than the telescopic fork, the Hossack system does not dive but rises.

In terms of shock absorption capabilities, the response of the three suspension systems is similar for road bump inputs regardless of their geometrical configuration, although some small differences can be observed between different systems. It has to be noted that Girder and Hossack suspensions were tuned to obtain the same equivalent stiffness and damping coefficient than those of the telescopic fork, despite these equivalent coefficients are not optimal values for the double wishbone suspension systems due to their particular designs. More precise responses would be achieved with individualized tuning of each suspension.

The results of stability analyses showed that different kinematic designs of a double wishbone suspension systems do not modify the motorcycle's stability. For each of the suspension systems (Girder and Hossack), the normal modes properties remain unaffected with the three geometrical configurations. However, these normal modes differ from one suspension system to the other. It was seen that normal modes behaviour depends on dynamic parameters, such as the front frame flexibility, the steering damping coefficient and the centre of mass location, in a similar manner for the Girder, Hossack and telescopic fork suspension systems. Although each suspension system presents its particular behaviour, general properties could be obtained for the three systems under study.

On one hand, variations on front frame compliance affect the motorcycle's stability in an opposite manner than the variations on the steering damper coefficient. Reducing twist rigidity results in decreased stability of the weave mode whilst the general wobble mode stability is improved. If the twist rigidity is increased, the wobble mode becomes less stable and the weave mode's stability is improved.

On the other hand, the centre of mass location with respect to the steering axis of the front frame has a remarkable impact on the motorcycle stability. For the three suspension systems under study, the weave and wobble modes' stability is improved if the centre of mass is displaced backwards. The wobble mode is observed to be more stable when the centre of mass is close to the steering axis, whilst displacing backwards the centre of mass over a certain limit reduces the stability of this mode.

In conclusion, both Girder and Hossack systems present interesting properties in terms of anti-dive and kinematic design that cannot be exploited with conventional telescopic fork suspensions. The different geometric configurations that can be obtained with these systems do not affect neither their shock absorption capabilities nor the stability of the motorcycle. However, the effect on the stability of dynamic properties such as centre of mass location or assembly's compliance have to be carefully considered in the design of these suspension systems.

References

1. Cooper, K.: The effects of aerodynamics on the performance and stability of high speed motorcycles. In: 2nd AIAA Symp. Aerodynamics Sport Competition Automobiles (1974)
2. Cossalter, V.: Motorcycle Dynamics, 2nd edn. Lulu.com, Morrisville (2006)
3. Dassault Systems: solidworks. www.solidworks.com. Accessed 20 Nov 2017
4. Evangelou, S.: The control and stability analysis of two-wheeled road vehicles. Ph.D. thesis, University of London (2003)
5. Evangelou, S., Limebeer, D., Tomas-Rodriguez, M.: Suppression of burst oscillations in racing motorcycles. In: 2010 49th IEEE Conference on Decision and Control (CDC), pp. 5578–5585 (2010)
6. Evangelou, S., Limebeer, D.J., Rodriguez, M.T.: Influence of road camber on motorcycle stability. J. Appl. Mech. **75**(6), 061020 (2008)
7. Evangelou, S., Limebeer, D.J.N., Sharp, R.S., Smith, M.C.: Mechanical steering compensators for high-performance motorcycles. J. Appl. Mech. **74**(2), 332–346 (2006)
8. Evangelou, S., Tomas-Rodriguez, M.: Motorcycle dynamic modes and passive steering compensation. In: Tanelli, M., Corno, M., Saveresi, S. (eds.) Modelling, Simulation and Control of Two-Wheeled Vehicles, 1st edn, pp. 221–241. Wiley, Hoboken (2014)
9. Evangelou, S.A., Limebeer, D.J.N., Tomas-Rodriguez, M.: Suppression of burst oscillations in racing motorcycles. J. Appl. Mech. **80**(1), 011003–011016 (2012)

10. Foale, T.: Motorcycle Handling and Chassis Design: The Art and Science, 2nd edn. Benidoleig, Alicante, Spain (2002)

11. Koenen, C.: The dynamic behaviour of motorcycles when running straight ahead and when cornering. Ph.D. thesis, Delft University of Technology (1983)

12. Limebeer, D.J.N., Sharp, R.S., Evangelou, S.: The stability of motorcycles under acceleration and braking. J. Mech. Eng. Sci. **215**(9), 1095–1109 (2001)

13. Mavroudakis, B., Eberhard, P.: Analysis of alternative front suspension systems for motorcycles. Veh. Syst. Dyn. **44**, 679–689 (2006)

14. Mechanical Simulation Corporation: VehicleSim technology. www.carsim.com. Accessed 20 Nov 2017

15. Pacejka, H.B.: Tire and Vehicle Dynamic, vol. 2, revised edn. Elsevier, Amsterdam (2002)

16. Pacejka, H.B., Bakker, E.: The magic formula tyre model. Veh. Syst. Dyn. **21**, 1–18 (1992)

17. Roe, G.E., Thorpe, T.E.: A solution of the low-speed wheel flutter instability in motorcycles. J. Mech. Eng. Sci. **18**(2), 57–65 (1976)

18. Shaeri, A., Limebeer, D.J.N., Sharp, R.S.: Nonlinear steering oscillations of motorcycles. In: 43rd IEEE Conference on Decision and Control, 2004. CDC, vol. 1, pp. 773–778 (2004)

19. Sharp, R.S., Evangelou, S., Limebeer, D.J.N.: Multibody aspects of motorcycle modelling with special reference to Autosim. In: Ambrósio, J.A.C. (ed.) Advances in Computational Multibody Systems, pp. 45–68. Springer, Dordrecht (2005)

20. Sharp, R.S.: The stability and control of motorcycles. J. Mech. Eng. Sci. **13**(5), 316–329 (1971)

21. Sharp, R.S.: Motorcycle steering control by road preview. J. Dyn. Syst. Meas. Control **129**(4), 373–382 (2007)

22. Sharp, R.S.: Rider control of a motorcycle near to its cornering limits. Veh. Syst. Dyn. **50**(8), 1–16 (2012)

23. Sharp, R.S., Evangelou, S., Limebeer, D.J.N.: Advances in the modelling of motorcycle dynamics. Multibody Syst. Dyn. **12**(3), 251–283 (2004)